

Gradual Domain Adaptation for Graph Learning

Pui Ieng Lei
University of Macau
Macau, China
yc37460@um.edu.mo

Ximing Chen
University of Macau
Macau, China
yc37921@um.edu.mo

Yijun Sheng
University of Macau
Macau, China
yc17419@um.edu.mo

Yanyan Liu
University of Macau
Macau, China
yc07402@um.edu.mo

Jingzhi Guo
University of Macau
Macau, China
jzguo@um.edu.mo

Zhiguo Gong
University of Macau
Macau, China
fstzgg@um.edu.mo

Abstract

Existing literature lacks a graph domain adaptation technique for handling large distribution shifts, primarily due to the difficulty in simulating an evolving path from source to target graph. To make a breakthrough, we present a *graph gradual domain adaptation* (GGDA) framework with the construction of a compact domain sequence that minimizes information loss in adaptations. Our approach starts with an efficient generation of knowledge-preserving intermediate graphs over the Fused Gromov-Wasserstein (FGW) metric. With the bridging data pool, GGDA domains are then constructed via a novel vertex-based domain progression, which comprises "close" vertex selections and adaptive domain advancement to enhance inter-domain information transferability. Theoretically, our framework concretizes the intractable inter-domain distance $W_p(\mu_t, \mu_{t+1})$ via implementable upper and lower bounds, enabling flexible adjustments of this metric for optimizing domain formation. Extensive experiments under various transfer scenarios validate the superior performance of our GGDA framework.

CCS Concepts

• **Networks** → **Network algorithms**.

Keywords

Graph Domain Adaptation; Gradual Knowledge Transfer

ACM Reference Format:

Pui Ieng Lei, Ximing Chen, Yijun Sheng, Yanyan Liu, Jingzhi Guo, and Zhiguo Gong. 2024. Gradual Domain Adaptation for Graph Learning. In *Proceedings of Make sure to enter the correct conference title from your rights confirmation email (Conference acronym 'XX)*. ACM, New York, NY, USA, 10 pages. <https://doi.org/XXXXXXX.XXXXXXX>

1 Introduction

Domain adaptation (DA) is a powerful solution for transferring knowledge from a label-rich (i.e., source) domain to a relevant

but label-scarce (i.e., target) domain under data distribution shifts [6, 24, 27, 38]. Recently, the intra-domain IID assumption faces challenges due to the explosive increase of non-IID data (e.g., social networks, traffic networks). This, along with the rapid development of graph neural networks (GNNs) [11, 17], urges the study of DA on graph-structured data. Unlike IID learning, a data representation in graph DA should encode information from both the individual data object (i.e. vertex) and its related objects (i.e. neighbors). A typical graph DA framework learns a graph encoder that captures data dependency via neighborhood aggregations while aligning source and target distributions in a latent space to enable knowledge transfer on a domain-invariant basis [20, 21, 33, 43, 44, 47]. However, theoretical analysis has shown that domain-invariant techniques perform poorly under a large discrepancy between source and target marginal distributions due to information distortion [51]. This issue is further exacerbated in non-IID scenarios, where data attributes and relations may shift jointly. Motivated by this, our paper delves into the critical challenge of graph DA under larger shifts. We follow an unsupervised DA (UDA) setting with a fully unlabeled target graph.

In IID-based UDA, to handle larger shifts, several algorithms incorporate unlabeled intermediate domains between source and target domains [13, 26, 36, 46]. Specifically, a line of research examines *gradual domain adaptation* (GDA), which leverages iterative model adaptations over a sequence of intermediate domains shifting from source to target [1, 3, 12, 18, 31, 41]. GDA turns a UDA problem with a large domain gap into several sub-UDA problems with small domain gaps, thereby bounding the generalization error of transfer. While intermediate data can sometimes be collected, e.g., portraits taken across years, in many cases, it is hard or even impossible to find suitable intermediate data. Accordingly, approaches such as interpolations and adversarial training have been employed to generate virtual intermediate data in IID-based UDA [1, 12, 26, 46].

Despite the promising performance of GDA, its applicability to non-IID graph-structured data remains unexplored due to the high intricacy involved. Aiming to advance graph DA performance under larger shifts, in this paper, we investigate a novel *graph gradual domain adaptation* (GGDA) framework from theoretical and empirical perspectives. Assuming no intermediate data is initially available, the central question here is: *In a non-IID context of graph-structured data, how should the intermediate domain sequence be constructed to ensure a high target accuracy from GGDA?*

Permission to make digital or hard copies of all or part of this work for personal or classroom use is granted without fee provided that copies are not made or distributed for profit or commercial advantage and that copies bear this notice and the full citation on the first page. Copyrights for components of this work owned by others than the author(s) must be honored. Abstracting with credit is permitted. To copy otherwise, or republish, to post on servers or to redistribute to lists, requires prior specific permission and/or a fee. Request permissions from permissions@acm.org.
Conference acronym 'XX, June 03–05, 2024, Woodstock, NY

© 2024 Copyright held by the owner/author(s). Publication rights licensed to ACM.
ACM ISBN 978-1-4503-XXXX-X/18/06
<https://doi.org/XXXXXXX.XXXXXXX>

To address this question, we first identify two key criteria: (1) intermediate domains should be constructed to *minimize information loss* upon GGDA, and (2) the construction scheme should allow *flexible adjustments* of the inter-domain Wasserstein distance, $W_p(\mu_t, \mu_{t+1})$, to enable a search for the optimal domain formation. In a graph context, primary challenges are twofold: (1) $W_p(\mu_t, \mu_{t+1})$ is inherently implicit as there is no explicitly defined structure space to accommodate all possible instance relations, and (2) the generation of every instance must account for both itself and neighbors.

Based on these considerations, we propose a novel GGDA framework as follows. We first develop an efficient technique to generate a sequence of intermediate graphs with weighted Fréchet mean over the Fused Gromov-Wasserstein (FGW) metric [37], a graph distance metric defined as the minimal cost of transporting both features and structures between two graphs. In this way, we avoid knowing the implicit cross-domain structure space. Our proposed entropy-guided matching, combined with coupling constraints in FGW computations, maximizes the infusion of valid knowledge from the given data into the generated data. Upon the generated data bridge, we introduce a novel domain progression scheme that constructs GGDA domains with enhanced inter-domain compactness for robust transfers. The scheme consists of two modules: regularized vertex selection for constructing a subsequent domain and adaptive mass decay for removing obsolete nodes from the current domain. By traversing the generated graphs and forming each domain with "close" vertices, the resulting cross-domain adaptation effectively preserves transferable and discriminative knowledge.

Theoretically, we demonstrate that the intractable $W_p(\mu_t, \mu_{t+1})$ is now concretized by its lower bound from the FGW metric and its upper bound from our vertex selection regularization. Moreover, a hyperparameter governing the scale of vertex selection under our prioritization enables flexible adjustments of $W_p(\mu_t, \mu_{t+1})$ without repetitive data generation. Here is a summary of our contributions:

- To the best of our knowledge, we are the first to investigate *gradual domain adaptation on graphs* (GGDA) and propose a solution tailored to *large domain gaps* in graph DA tasks.
- Our GGDA framework constructs a compact domain sequence for stable inter-graph knowledge transfer. We tackle the non-trivial issue of structure implicitness by designing tractable modules with theoretical bounding effects.
- Extensive experiments on fifteen datasets validate the effectiveness of our GGDA framework. In particular, our framework beats the best baseline by an average of +5.02%.

2 Preliminaries

2.1 Notations

A simplex of n bins is denoted by $\Sigma_n = \{h \in \mathbb{R}_+^n \mid \sum_i h_i = 1\}$. For two histograms $h \in \Sigma_n$ and $h' \in \Sigma_m$, we denote the set of all couplings between h and h' by $\Pi(h, h') = \{\pi \in \mathbb{R}_+^{n \times m} \mid \sum_i \pi_{i,j} = h'_j; \sum_j \pi_{i,j} = h_i\}$. For a space Ω and $x \in \Omega$, δ_x denotes the Dirac measure in x . The support of probability measure $\mu \in P(\Omega)$ is denoted by $\text{supp}(\mu) = \text{argmin}_A \{|A| \mid A \subset \Omega; \mu(\Omega \setminus A) = 0\}$.

2.2 Graph Space

In this paper, any graph is viewed as a distribution sampled from a product space of features and structures. An undirected attributed graph $\mathcal{G} = (\mathcal{V}, \mathcal{E})$ contains the set of vertices \mathcal{V} and edges \mathcal{E} . Each vertex $v_i \in \mathcal{V}$ has (1) a feature representation x_i in some space (Ω_x, d_x) and (2) a structure representation a_i in some space (Ω_a, C) . In practice, Ω_a is implicit, and $C : \Omega_a \times \Omega_a \rightarrow \mathbb{R}_+$ measures the similarity between pairs of nodes in terms of their structures in the graph. In general, C can encode the node neighborhood information (e.g., node adjacency) or the distance between nodes (e.g., shortest path). Note that the integration of space Ω_a indicates that samples (i.e., vertices) are not IID anymore. For a graph with n vertices, a histogram $h \in \Sigma_n$ describes each vertex's relative importance within the graph (e.g., uniform or degree distribution). This allows the graph to be represented as $\mu = \sum_{i=1}^n h_i \delta_{(x_i, a_i)}$, a fully supported probability measure over the product space $\Omega_x \times \Omega_a$. Given that all nodes have an underlying label $y_i \in \Omega_y$, the graph can be extended to the product space $\Omega_x \times \Omega_a \times \Omega_y$, i.e., $\mu = \sum_{i=1}^n h_i \delta_{(x_i, a_i, y_i)}$.

2.3 Models and Objectives

Consider a node classification task, where the goal is to predict node labels given node features and graph topology. For simplicity, we present the case of binary classifications with node labels $y_i \in \{-1, 1\}$ and $\Omega_y := \mathbb{R}$. Given a model family Θ , for each $\theta \in \Theta$, a model $M_\theta : \Omega_x \times \Omega_a \rightarrow \Omega_y$ outputs the classification predictions. Each model can be viewed as a composite function with respect to some Euclidean embedding space (Ω_z, d_z) , i.e., $M_\theta = \Psi_\theta \circ \Phi_\theta$, where $\Phi_\theta : \Omega_x \times \Omega_a \rightarrow \Omega_z$ (e.g., GNN encoder) and $\Psi_\theta : \Omega_z \rightarrow \Omega_y$.

Consider $T + 1$ graph distributions (i.e., domains), denoted by $\mu_0, \mu_1, \dots, \mu_T$. For unsupervised graph DA, $\mu_0 = \mu_S$ is a fully-labeled source domain and μ_T is a fully-unlabeled target domain. For GGDA, μ_1, \dots, μ_{T-1} are unknown intermediate domains transitioning from source to target. The population loss in t -th domain is defined as

$$\epsilon_t(\theta) \equiv \epsilon_{\mu_t}(\theta) = \mathbb{E}_{x,a,y \sim \mu_t} [\ell(M_\theta(x, a), y)], \quad (1)$$

where ℓ is the loss function. The goal is to find a model M_θ that yields a low classification error on the target graph, i.e., low $\epsilon_T(\theta)$.

3 Analysis of GGDA Domain Generation

Our goal is to transfer knowledge between the relevant source and target graphs under a large distribution shift. While no intermediate data is available, we aim to generate intermediate domains appropriately to promote a stable long-range knowledge transfer. Assumptions and proofs for this paper can be found in the appendix.

The first important consideration is the criteria that intermediate domains should satisfy such that the target error from GGDA on the domain sequence is well-bounded. Previous GDA work has shown from an online learning perspective that the generalization error of gradual domain adaptation can be bounded as [41]

$$\epsilon_T(\theta_T) \leq \epsilon_0(\theta_0) + \mathcal{O}\left(T\Delta + \frac{T}{\sqrt{n}}\right) + \tilde{\mathcal{O}}\left(\frac{1}{\sqrt{nT}}\right). \quad (2)$$

This bound still holds in our non-IID setting under mild assumptions (see appendix). In a graph context, n indicates the average number

of vertices in each domain, and

$$\Delta = \frac{1}{T} \sum_{t=0}^{T-1} W_p(\mu_t, \mu_{t+1}), \quad (3)$$

where $\mu_t = \sum_{i=1}^{n_t} h_i^t \delta_{(x_i^t, a_i^t, y_i^t)}$ and W_p is the p-Wasserstein distance. Meanwhile, there is an inverse relationship between the optimal Δ and T [41], suggesting that when the average distance between consecutive domains is large, the number of intermediate domains should be fewer, and vice versa. Note that this does not imply that the bound is tightest at $T = 1$ (i.e., non-GDA). In fact, based on Eq. 2 as well as past empirical GDA studies [18, 41], the optimal performance is typically achieved at a "sweet spot" when T is moderately large (i.e., Δ is moderately small). This further underscores the need for a GDA algorithm on graphs to divide a large shift into multiple smaller shifts to enhance adaptation performance.

Given the above analysis, we conclude two criteria that the intermediate domain generation should satisfy for a successful GGDA: (1) the length of the path connecting source and target, i.e., $T\Delta$, should be small; and (2) a search for the optimal Δ should be conducted under an inverse relationship between Δ and T . To fulfill these criteria, there are three main challenges as follows:

- (1) Both criteria necessitate domain generation according to inter-domain distance $W_p(\mu_t, \mu_{t+1})$ over $\Omega_x \times \Omega_a \times \Omega_y$. This is non-trivial since (i) $W_p(\mu_t, \mu_{t+1})$ over Ω_a is inherently implicit, and (ii) during generation, each created sample (i.e., vertex) within domain μ should be characterized not only by its own information but also by that of its neighbors.
- (2) For criterion (1), an ideal solution is to generate a Wasserstein geodesic over $\Omega_x \times \Omega_a \times \Omega_y$, yet this is extremely challenging in practice due to the intractable optimization for an exact geodesic of attributed topological data.
- (3) While the p-Wasserstein metric is defined on $\Omega_x \times \Omega_a \times \Omega_y$, only the source domain is labeled. How the intermediate domains should be generated to effectively integrate class information (i.e., y -dimension) poses another key challenge.

To tackle challenge (1), we propose to facilitate domain generation through concretization of graph metric (especially over the implicit topology on Ω_a) by leveraging the FGW distance as a bridge between abstract distance W_p and practical implementations. Regarding challenge (2), we refine the concept of geodesic into a practical realization in this setting: *minimizing information loss during the GGDA process*. Specifically, we aim to approximate the shortest path between source and target with intermediate domains that minimize information loss upon model adaptations. This is achieved by a combination of FGW optimizations and a subsequent vertex selection process for domain constructions. Additionally, the vertex selection process addresses challenge (3) via enhanced pseudo-labeling for domain progression. In the following sections, we will provide the detailed explanations accordingly.

4 Graph Generation over FGW Metric

While we wish to generate intermediate domains that adhere to the distance defined in Eq. 3, a primary challenge is that $W_p(\mu_t, \mu_{t+1})$ over the product space $\Omega_x \times \Omega_a \times \Omega_y$ is intractable, as the metric for measuring the structural distance between cross-graph samples over Ω_a is implicit (i.e., no inter-graph edges), which presents a

dilemma specific to a non-IID context. To bridge the gap between theoretical insights and practical implementations, we require a well-defined and tractable inter-graph distribution distance that considers both features and structures. To this end, we adopt the Fused Gromov-Wasserstein (FGW) distance defined as follows.

Definition 1. (FGW distance) Let two attributed graphs be $\mu = \sum_{i=1}^n h_i \delta_{(x_i, a_i)}$ and $\nu = \sum_{j=1}^m h'_j \delta_{(x'_j, a'_j)}$. Let $d_x(i, j) = d_x(x_i, x'_j)$ be the distance between cross-network features, while $C(i, k) = C(a_i, a_k)$ and $C'(j, l) = C'(a'_j, a'_l)$ are the respective structure matrix for μ and ν . Given the set of all admissible couplings $\Pi(h, h')$ and $\alpha \in [0, 1]$, the FGW distance in the discrete case is defined as [37]

$$\begin{aligned} FGW_{\alpha, p, q}(\mu, \nu) &= \left(\min_{\pi \in \Pi(h, h')} E_{\alpha, p, q}(\pi) \right)^{\frac{1}{p}}, \quad \text{where} \\ E_{\alpha, p, q}(\pi) &= \sum_{i, j, k, l} \left[(1 - \alpha) d_x(i, j)^q \right. \\ &\quad \left. + \alpha |C(i, k) - C'(j, l)|^q \right]^p \pi_{i, j} \pi_{k, l}. \end{aligned} \quad (4)$$

$E(\pi)$ is the cost of transporting between graphs with node matching strategy π , which includes the costs of transporting features across single nodes and transporting structures across pairs of nodes. The FGW distance is the minimal cost given by the optimal coupling. Hence, the computation of FGW is built upon sample coupling that preserves both feature and relation similarities. Under such constraints, node i is matched to node j only if they have similar features and their neighbors (i.e., k, l) also present a correspondence.

4.1 Fast Entropy-Guided Graph Generation

Having defined an implementable graph metric, we now proceed to generate the intermediate graphs for bridging the gap between source and target graphs. Note that at this stage, "intermediate graphs" do not yet refer to "intermediate domains". We propose to generate a sequence of $K - 1$ intermediate graphs $\{\tilde{\mu}_k\}_{k=1}^{K-1}$ via the weighted Fréchet mean [39] over the FGW metric on $\Omega_x \times \Omega_a$ (without Ω_y as μ_T is unlabeled). However, directly computing the Fréchet mean between the *entire* source and target graphs can be costly, especially in the case of large graphs. To enhance both efficiency and knowledge preservation, we introduce a partition-based, entropy-guided graph generation strategy, where each intermediate graph $\tilde{\mu}_k$ is generated as a combination of smaller graphs $\{\tilde{\mu}_{k_i}\}_i$.

To begin with, we transform the source and target graphs into P_S and P_T partitions with METIS [16], an algorithm that minimizes the number of cross-partition edges. Then, the overall idea is to generate each $\tilde{\mu}_{k_i}$ using a pair of source and target partitions, denoted by $\hat{\mu}_{m(P_t)}^S$ and $\hat{\mu}_{P_t}^T$, with indices $m(P_t) \in \{1, 2, \dots, P_S\}$ and $P_t \in \{1, 2, \dots, P_T\}$. The function $m(\cdot)$ represents an index matching between source and target partitions, which we aim to optimize to enhance knowledge preservation during graph generation.

To achieve this, we first initiate a warm-up phase to obtain a preliminary matching $\hat{m}(\cdot)$ before graph generation. Let $m(\cdot)$ be a random matching, $n_{m(P_t)}^S$ and $n_{P_t}^T$ be the size of the partition pair, $\Upsilon_{m(P_t), c}^S \in \{0, 1\}^{n_{m(P_t)}^S}$ be an indicator of source nodes belonging to class $c \in \{-1, 1\}$, and $\pi^*(m(P_t), P_t) \in [0, 1]^{n_{m(P_t)}^S \times n_{P_t}^T}$ be the

normalized FGW optimal coupling on $\Omega_x \times \Omega_a$ between the partition pair. Then, for each $P_t \in \{1, 2, \dots, P_T\}$, compute the following:

$$\begin{aligned} f_{(m(P_t), P_t), c} &= \left[\text{diag}(Y_{m(P_t), c}^S) \cdot \pi^*(m(P_t), P_t) \right]^T \cdot \mathbf{1}, \\ F_{(m(P_t), P_t)} &= \left[f_{(m(P_t), P_t), -1}, f_{(m(P_t), P_t), 1} \right], \\ H_{(m(P_t), P_t)} &= \frac{1}{n_{P_t}^T} \sum_{i=1}^{n_{P_t}^T} \left[- \sum_j F_{(m(P_t), P_t), ij} \cdot \log F_{(m(P_t), P_t), ij} \right]. \end{aligned} \quad (5)$$

Here $F_{(m(P_t), P_t)} \in [0, 1]^{n_{P_t}^T \times 2}$ contains each target node's push-forward class distribution, and $H_{(m(P_t), P_t)} \in \mathbb{R}$ is the average target node class entropy. While such class distribution is only a broad estimation, it is a useful indicator of information compatibility between the pair $(m(P_t), P_t)$, i.e., a large H indicates that much valid class information has been lost by coupling this pair over FGW. Combining the effects of source class entropy H^S and FGW distance, for each pair $(m(P_t), P_t)$, we derive a measure of information loss

$$S_{\text{loss}}(m(P_t), P_t) = \left(H_{(m(P_t), P_t)} / H_{m(P_t)}^S \right) \cdot \text{FGW}(\hat{\mu}_{m(P_t)}^S, \hat{\mu}_{P_t}^T), \quad (6)$$

where all components are normalized. During the warm-up phase, different randomizations of $m(\cdot)$ are employed, and a preliminary matching is set to $\hat{m}(P_t) = \text{argmin}_{m(P_t) \in \mathcal{M}_{\text{random}}(P_t)} S_{\text{loss}}(m(P_t), P_t)$.

We now proceed to knowledge-preserving graph generation with matched partition pairs. In this phase, $m(P_t)$ is set to $\hat{m}(P_t)$ with a probability $\propto 1/S_{\text{loss}}(\hat{m}(P_t), P_t)$ and is set to a random matching otherwise. With this matching strategy, we generate a sequence of unlabeled intermediate graphs $\{\tilde{\mu}_k\}_{k=1}^{K-1}$ over $\Omega_x \times \Omega_a$ via the following weighted Fréchet mean optimization for each k :

$$\tilde{\mu}_k = \frac{1}{\Gamma} \sum_i \tilde{\mu}_{k,i} \left|_{\tilde{\mu}_{k,i} = \text{argmin}_{\mu} \left[\left(\frac{K-k}{K} \right) \cdot \text{FGW}(\mu, \hat{\mu}_{m(P_t,i)}^S) + \left(\frac{k}{K} \right) \cdot \text{FGW}(\mu, \hat{\mu}_{P_t,i}^T) \right]} \right. \quad (7)$$

where $P_{t,i} \sim \text{Uniform}\{1, 2, \dots, P_T\}$ and Γ is a normalizing factor. This scheme constructs a bridging graph sequence $\{\tilde{\mu}_k\}_{k=1}^{K-1}$ by incrementally shifting the position of $\tilde{\mu}_k$ between μ_S and μ_T over the FGW metric. Meanwhile, the index matching $\hat{m}(\cdot)$ is continuously refined whenever a new matching yields a smaller S_{loss} than the previous one. In this phase, $S_{\text{loss}}(m(P_t), P_t)$ is computed by substituting (1) the source-intermediate optimal coupling $\pi^*(m(P_{t,i}), k_i)$ in Eq. 5 and (2) the distance sum $\text{FGW}(\hat{\mu}_{m(P_{t,i})}^S, \tilde{\mu}_{k,i}) + \text{FGW}(\tilde{\mu}_{k,i}, \hat{\mu}_{P_{t,i}}^T)$ in Eq. 6, both obtained directly from Fréchet mean optimization, i.e., no extra computations. Since the entropy reflecting information loss is now evaluated on $\tilde{\mu}_{k,i}$, the information integrity within the generated intermediate graphs can be further boosted. Overall, with our accelerated module, the time complexity of graph generation largely reduces from $\mathcal{O}(\bar{n}^3)$ to $\mathcal{O}(\bar{P}\bar{n}^3)$ (see appendix).

4.2 Analysis: Why Is FGW-Based Graph Generation Important?

While the FGW-generated graphs do not inherently conform to $W_p(\mu_t, \mu_{t+1})$ over $\Omega_x \times \Omega_a \times \Omega_y$ in Eq. 3, this proposed generation process is central to our algorithm for two reasons.

First, the minimization in Eq. 7 serves as a mechanism of information preservation in the construction of intermediate graphs by aiming to reduce the FGW distance between $\tilde{\mu}_{k_i}$ and $\hat{\mu}_S/\hat{\mu}_T$. The sample correspondence constraint inherent in FGW optimization drives the ego-graphs distributed in the generated $\tilde{\mu}_k$ to preserve and combine the characteristics of source and target ego-graphs. In other words, this approach serves to *minimize the information loss* over $\Omega_x \times \Omega_a$ when generating the bridging data sequence.

Second, as discussed in Section 3, the domain generation should be conducted by searching for an optimal $W_p(\mu_t, \mu_{t+1})$ over $\Omega_x \times \Omega_a \times \Omega_y$. While this W_p distance is intractable, it is, in fact, lower bounded by the FGW distance over $\Omega_x \times \Omega_a$, as shown below.

Proposition 2. For graph measures $\mu(x, a, y) = \sum_{i=1}^n h_i \delta_{(x_i, a_i, y_i)}$ and $\nu(x', a', y') = \sum_{j=1}^m h'_j \delta_{(x'_j, a'_j, y'_j)}$, along with their marginal measures $\mu(x, a) = \sum_{i=1}^n h_i \delta_{(x_i, a_i)}$ and $\nu(x', a') = \sum_{j=1}^m h'_j \delta_{(x'_j, a'_j)}$,

$$W_p(\mu(x, a, y), \nu(x', a', y')) \geq \text{FGW}_{\alpha, p, 1}(\mu(x, a), \nu(x', a'))/2. \quad (8)$$

This relation implies that, in order to generate data with a certain W_p distance, a necessary condition is to reduce the FGW distance between the data. Intuitively, it means that the presence of generated data with a small FGW distance is crucial for establishing a data pool that enables subsequent refinements for achieving the desired $W_p(\mu_t, \mu_{t+1})$ and, ultimately, a successful GGDA process.

5 Domain Construction and GGDA

Gradual domain adaptation (GDA) involves model training on a sequence of T domains with labeled data, such that the model shifts from source domain μ_0 to target domain μ_T with small steps over the intermediate domains $\{\mu_t\}_{t=1}^{T-1}$. Specifically, since only the source domain contains ground-truth labels, each intermediate domain is defined with pseudo-labels obtained during iterative training. To perform GDA on graphs, one major consideration, as discussed above, is how to properly define the intermediate domain sequence over $\Omega_x \times \Omega_a \times \Omega_y$ to minimize information loss during the GGDA process. Specifically, it is crucial to ensure that pseudo-labeling can be performed accurately when defining each labeled intermediate domain under our algorithm, such that the label accuracy decay over the entire GGDA process can be well restrained.

5.1 Analysis: Vertex-Based Domain Construction for GGDA

Given the FGW-generated graph sequence, it might be tempting to define each *intermediate domain* μ_t as a single *intermediate graph* $\tilde{\mu}_k|_{k=t}$ with post-assigned pseudo-labels. However, such a definition is not optimal, as the FGW distance itself is not an upper bound of $|\epsilon_{k+1}(\theta) - \epsilon_k(\theta)|$, i.e., it does not inherently ensure information transferability (and thus the correctness of pseudo-labeling) from $\tilde{\mu}_k$ to $\tilde{\mu}_{k+1}$. To this end, we propose to construct each domain μ_t progressively along the training by selecting vertices from the data pool. This method offers two key advantages as described below.

First, the final task of GGDA is vertex-based (i.e., node classification), focusing on the characteristics of each vertex encoded in its ego-graph. Therefore, rather than directly using a complete FGW-generated graph as an individual domain, defining each subsequent

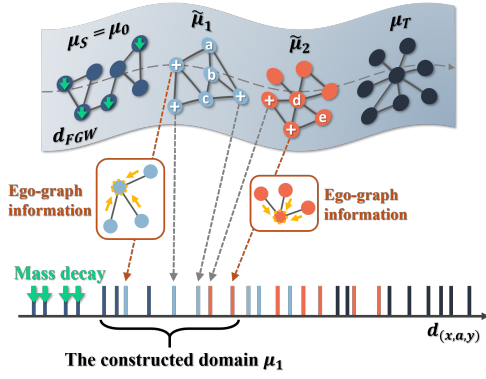


Figure 1: Illustration highlighting the rationale of our GGDA framework. The upper part shows the generated graph sequence over FGW metric, and the lower part shows the corresponding vertex relations over product space distance $d_{(x,a,y)}$. μ_0 (in dark blue) is initially labeled. "+" indicates added vertices and green lower arrow indicates downweighted vertices.

domain as a set of vertices selected based on their encoded knowledge relative to vertices from the previous domain better preserves the transferable and discriminative knowledge during adaptation. As presented in Figure 1, assume we start with the labeled domain $\mu_S = \mu_0$ for the training. Since vertices within the graph sequence inherently possess different relevance to μ_0 in terms of the $d_{(x,a,y)}$ metric (i.e., distance over $\Omega_x \times \Omega_a \times \Omega_y$), if we manage to select vertices close to μ_0 (marked with "+") from the data sequence for constructing the subsequent domain μ_1 , the resulting cross-domain knowledge transfer can be enhanced by minimal information loss.

Second, since the newly constructed domain can contain vertices from different graphs, the domain's connections to unused vertices in the pool are naturally maintained through existing edges. Knowledge propagation upon these edges improves the correctness of pseudo-labeling on linked vertices and, thus, the quality of the next constructed domain. Put differently, the existence of inter-domain edges is the key to a successful GGDA as it signifies a higher domain transfer potential and a smaller information loss between consecutive domains. In Figure 1, consider vertices marked with "+" being correctly pseudo-labeled and included in domain μ_1 . In this case, vertices a to e , as prospective components of domain μ_2 , can be assigned accurate pseudo-labels by gathering reliable messages directly from their labeled neighbors. Such an insight regarding inter-domain connectivity can also be stated from a theoretical perspective, as illustrated in the following proposition.

Proposition 3. Consider graph domains $\mu = \sum_{i=1}^n h_i \delta_{(x_i, a_i, y_i)}$ and $\nu = \sum_{j=1}^m h'_j \delta_{(x'_j, a'_j, y'_j)}$ with uniform weights h and h' . Let \mathcal{E} be the set of unit-weight edges linking μ and ν and $\tilde{\pi}$ be an arbitrary coupling satisfying $\tilde{\pi}_{i,j} = \frac{1}{nm} \mathbb{1}_{\{(i,j) \in \mathcal{E}\}}$. For any $\theta \in \Theta$,

the population loss on μ and ν given by M_θ satisfies

$$|\epsilon_\mu(\theta) - \epsilon_\nu(\theta)| \leq \rho(\zeta_1 + \zeta_2), \quad \text{where}$$

$$\zeta_1 = \frac{\sqrt{\tilde{R}^2 + 1}}{n \cdot m} \sum_{(i,j) \in \mathcal{E}} \left(\|z_i(\theta) - z'_j(\theta)\| + |y_i - y'_j| \right), \quad (9)$$

$$\zeta_2 = \sqrt{\tilde{R}^2 + 1} \left[\min_{\tilde{\pi}} \left(\sum_{(i,j) \notin \mathcal{E}} d_{(x,a,y)} \left((x_i, a_i, y_i), (x'_j, a'_j, y'_j) \right)^P \cdot \tilde{\pi}_{i,j} \right) \right]^{\frac{1}{P}}.$$

When transferring a model between arbitrary graph domains μ and ν , the error bound consists of two components (i.e., ζ_1 and ζ_2) regarding node pairs *with* and *without* inter-domain edges. For ζ_1 , $\sum_{(i,j) \in \mathcal{E}} \|z_i(\theta) - z'_j(\theta)\|$ is small as most GNNs act as a graph Laplacian regularization that constrains the learned embeddings of two connected nodes to be similar [53]. Meanwhile, $\sum_{(i,j) \in \mathcal{E}} |y_i - y'_j|$ is small if the graphs are homophilic. For ζ_2 , however, the distance $\sum_{(i,j) \notin \mathcal{E}} d_{(x,a,y)}^P$ can be unbounded. We therefore expect a tighter bound when consecutive domains are not mutually isolated.

5.2 The Domain Progression Framework

Motivated by the analysis, we propose a GGDA framework with the domain sequence $\{\mu_t\}_{t=0}^T$ constructed progressively in a vertex-based manner along the training. Specifically, given the current domain, we define the subsequent domain with two novel modules: regularized vertex selection and adaptive mass decay.

Let $|M_\theta(x, a)|$ be the geometric margin and $\text{sign}(M_\theta(x, a))$ be the prediction, respectively. Further, we consider the entire generated graph sequence as a single batched graph μ_B over $\Omega_x \times \Omega_a$, where $\mathcal{V}_B := \text{supp}(\mu_B) = \bigcup_{k=1}^{K-1} \text{supp}(\tilde{\mu}_k) \cup \text{supp}(\mu_S) \cup \text{supp}(\mu_T)$, and we initialize a mass decay mask $w_{v_b}^0 = 1$ for all $v_b \in \mathcal{V}_B$. At first, only nodes from the source graph are labeled, so we define $\mu_0 = \mu_S = \sum_{i=1}^{n_S} h_i^S \delta_{(x_i^S, a_i^S, y_i^S)}$ with $h_i^S = 1/n_S$. In each upcoming iteration, we perform the two modules below to construct the subsequent domain μ_{t+1} and shift the model from μ_t to μ_{t+1} .¹

5.2.1 Vertex Selection for Constructing Next Domain. Let $\mathcal{V}_t^t := \text{supp}(\mu_t)$ denote the set of vertices of the current domain μ_t and $\mathcal{V}_u^t := \mathcal{V}_B \setminus (\bigcup_{t'=0}^t \mathcal{V}_t^{t'})$ be the set of unused vertices within the data sequence. First, we train a new model θ_t on the current domain μ_t with loss $\mathbb{E}_{x,a,\hat{y} \sim \mu_t} [\ell(M_{\theta_t}(x, a), \hat{y})] = \sum_{v_l \in \mathcal{V}_t^t} h_l^t \cdot \ell(M_{\theta_t}(x_l, a_l), \hat{y}_l)$, where \hat{y} is either a pseudo-label or a ground-truth label. In the inference phase, for each $v_u \in \mathcal{V}_u^t$, compute the regularized score

$$c_u^t = |M_{\theta_t}(x_u, a_u)| \cdot \exp\left(-\frac{d_u^t}{\max_{\{v_{u'} \in \mathcal{V}_u^t\}} d_{u'}^t} \cdot \eta\right), \quad (10)$$

$$\text{where } d_u^t = \min_{v_l \in \mathcal{V}_l^t} d_z(\Phi_{\theta_t}(x_u, a_u), \Phi_{\theta_t}(x_l, a_l)).$$

Here d_z is the Euclidean distance. In this module, we first obtain the node embeddings by aggregating the feature and structure information of each vertex encoded in its ego-graph, which is either given or generated over the FGW metric. Then, an η -penalty mechanism prioritizes vertices with high classification confidence within the embedding neighborhood of μ_t . Specifically, vertices are sorted by c_u^t and selected within a constraint κ , the ratio of the number of new

¹From here till the end of section 5.2, we denote $(x_{v_n}, a_{v_n}, \hat{y}_{v_n}, h_{v_n}, w_{v_n})$ by $(x_n, a_n, \hat{y}_n, h_n, w_n)$.

pseudo-labels per class to the number of source labels per class. The selected vertex set, denoted by \mathcal{V}_{pl}^t , will be included in the next domain μ_{t+1} with sharpened pseudo-labels $\hat{y}_{pl} = \text{sign}(M_{\theta_t}(x_{pl}, a_{pl}))$ for $v_{pl} \in \mathcal{V}_{pl}^t$. To illustrate the rationale behind this module, we present the following proposition.

Proposition 4. Let $\Phi_{\tilde{\theta}} : \Omega_x \times \Omega_a \rightarrow \Omega_z$ be an (L, γ) -quasiisometric graph embedding [5]. Let $\mu(z|\tilde{\theta}) = \sum_{i=1}^n h_i \delta_{z_i|\tilde{\theta}}$, $\nu(z'|\tilde{\theta}) = \sum_{j=1}^m h'_j \delta_{z'_j|\tilde{\theta}}$, and $\pi^* = \text{argmin}_{\pi \in \Pi(h, h')} \sum_{i,j} d_z(z_i|\tilde{\theta}, z'_j|\tilde{\theta})^p \pi_{i,j}$. Then we have

$$W_p(\mu(x, a, y), \nu(x', a', y')) \leq \xi \text{ and } |\epsilon_\mu(\theta) - \epsilon_\nu(\theta)| \cdot \mathcal{O}(\rho^{-1}) \leq \xi,$$

$$\text{where } \xi = \left[W_\infty(\mu(z|\tilde{\theta}), \nu(z'|\tilde{\theta})) + \gamma + \frac{1}{L} \left(\sum_{i,j} |y_i - y'_j|^p \pi_{i,j}^* \right)^{\frac{1}{p}} \right]. \quad (11)$$

From Proposition 4, two conclusions in relation to our approach can be drawn: (1) Under the covariate shift assumption, our vertex selection strategy based on the sorted score c_u^t adheres to ξ by prioritizing samples that are within the Ω_z neighborhood and distant from the decision boundary. Therefore, modifying κ , which controls the scale of class-unbiased vertex selection under c_u^t -prioritization, enables flexible adjustment of $W_p(\mu_t, \mu_{t+1})$ over $\Omega_x \times \Omega_a \times \Omega_y$ via its upper bound ξ while satisfying an inverse relationship between Δ and T , i.e., realization of an efficient global search for optimal GGDA domain path formation without requiring any repetitive data generation. (2) Meanwhile, since our proposed prioritization favors the selection of vertices close to μ_t over the implicit metric $d_{(x,a,y)}$ for inclusion in the next domain μ_{t+1} , it ensures *minimal information loss* by largely preserving transferrable and discriminative knowledge from μ_t to μ_{t+1} , thereby establishing a bounding effect on the local generalization error $|\epsilon_\mu(\theta) - \epsilon_\nu(\theta)|$.

5.2.2 Adaptive Mass Decay of Vertices. Given the stochasticity in \mathcal{V}_{pl}^t , strictly excluding all vertices \mathcal{V}_l^t from \mathcal{V}_l^{t+1} may result in low inter-domain connectivity in the succeeding iteration, degrading pseudo-label quality. Moreover, since a new model is trained in every domain, significantly more generated data is required if each domain contains only new vertices, which is inefficient. To this end, we propose an adaptive decay on the distribution mass of \mathcal{V}_l^t . Let the set of labeled nodes be $\mathcal{V}_{pll}^t := \mathcal{V}_l^t \cup \mathcal{V}_{pl}^t$. In every iteration, we store the label score $\hat{c}_{pll}^t = \hat{y}_{pll} \cdot M_{\theta_t}(x_{pll}, a_{pll})$ for $v_{pll} \in \mathcal{V}_{pll}^t$. Then, if $t \geq 1$, we compute the mass decay for $v_l \in \mathcal{V}_l^t$ as

$$\lambda_l^t = \exp\left(-\left[1 - \min\left(\frac{\hat{y}_l \cdot M_{\theta_t}(x_l, a_l)}{\hat{c}_l^{t-1}}, 1\right)\right] \cdot \beta\right). \quad (12)$$

This computation identifies the model flow after training in a new domain by quantifying label correctness degradation. Nodes with degraded labels will be downweighted in the next constructed domain to promote model advancement, with β regulating the mass decay level. Accordingly, we update the mask $w_l^t = w_l^{t-1} \cdot \lambda_l^t$ for

$v_l \in \mathcal{V}_l^t$ cumulatively and define the next domain distribution as

$$\begin{aligned} \mu_{t+1} &= \frac{1}{\Gamma} \left(\sum_{v_l \in \mathcal{V}_l^t} w_l^t \cdot \delta_{(x_l, a_l, \hat{y}_l)} + \sum_{v_{pl} \in \mathcal{V}_{pl}^t} \delta_{(x_{pl}, a_{pl}, \hat{y}_{pl})} \right) \\ &= \sum_{v_{pll} \in \mathcal{V}_{pll}^t} h_{pll}^{t+1} \cdot \delta_{(x_{pll}, a_{pll}, \hat{y}_{pll})}, \end{aligned} \quad (13)$$

where Γ is a normalizing factor such that $\sum h_{pll}^{t+1} = 1$. In practice, we can keep only the top- k weighted samples in $\text{supp}(\mu_{t+1})$ and assign a mass of 0 to others, with k being the average size of source and target graphs. The decay technique is conceptually illustrated in Figure 1, with a minor distinction that this technique takes effect only when $t \geq 1$ (i.e., starting from the construction of μ_2). Note that while some target vertices might be labeled prior to the final stage, mass decay is not applied to these vertices as our goal is to adapt to the target graph. The GGDA process concludes with one final training when sufficient target vertices are confidently labeled.

6 Experiments

Our goal is to examine whether our GGDA framework with the constructed domain sequence improves graph knowledge transfer. We focus on cross-network node classifications, with source labels used for training and target labels used for validation and testing under a 2:8 ratio [21]. Additional experiments, implementation details, data statistics, etc. are provided in the appendix.

6.1 Datasets

For datasets within the following four groups, we use one as source and the other as target. (1) **ACM** (pre-2008), **Citation** (post-2010), and **DBLP** (2004 to 2008) (denoted by **A, C, D**): multi-label citation networks extracted from ArnetMiner [33]; (2) **ACM2** (2000 to 2010) and **DBLP2** (post-2010), (denoted by **A2, D2**): another pre-processed version of single-label citation networks [44]; (3) **Blog1** and **Blog2** (denoted by **B1, B2**): social networks from BlogCatalog, with 30% of the binary attributes randomly flipped to enlarge discrepancy [19]; (4) **Arxiv 2007, 2016, 2018**: Arxiv computer science citation networks partitioned by time (all from the year 1950) [14].

For citation networks **Cora** and **CiteSeer** [32], as well as Twitch social networks **ENGB, DE, and PTBR** [30], we simulate a *multi-step shifting process* independently on each graph to mimic gradual data shifts. Specifically, we perform 5 steps of class-wise feature shifts generated with Gaussian noise. This effectively shifts the distribution in $\Omega_x \times \Omega_a \times \Omega_y$ since both $p(a|x)$ and $p(x|y)$ have changed accordingly. These datasets with multi-step shifting will be used for evaluation in different ways, as detailed later.

6.2 Baselines

We compare our GGDA framework with the following baselines: **CDAN** [23], **MDD** [49], **UDA-GCN** [44], **ACDNE** [33], **ASN** [48], **GRADE** [43], **StruRW** [21], **SpecReg** [47], **GraphAlign** [15], and **A2GNN** [20]. Specifically, CDAN and MDD are non-graph DA methods, for which we replace the encoder with GCN [17]. All other baselines are graph DA methods under the **domain-invariant representation (DIR)** framework, except for GraphAlign, which is the first data-centric graph DA method introduced recently. While

Table 1: Micro-F1 and macro-F1 scores (i.e., F1MI and F1MA) of node classifications on the target graph.

	A to C		A to D		C to A		C to D		D to A		D to C		Δ_{Mean}
	F1MI	F1MA	F1MI	F1MA	F1MI	F1MA	F1MI	F1MA	F1MI	F1MA	F1MI	F1MA	
CDAN	77.4±0.3	74.7±0.5	69.6±0.5	65.3±1.5	73.7±0.3	72.5±0.5	73.9±0.3	70.9±0.6	69.0±0.4	66.3±0.7	74.3±0.3	70.8±0.6	+0.4
MDD	76.4±0.4	72.9±0.7	67.6±0.6	61.2±1.6	74.5±0.5	73.4±0.7	73.2±0.4	70.2±0.5	69.8±0.4	66.6±0.8	74.5±0.5	70.3±0.9	-0.3
UDA-GCN	74.0±0.7	71.2±1.5	69.0±0.8	61.3±2.4	72.6±0.5	71.4±0.6	71.5±0.6	66.0±2.7	70.4±0.7	67.7±2.3	74.5±0.4	71.0±1.1	-1.1
ACDNE	78.9±0.3	77.3±0.3	72.2±0.3	69.9±0.3	76.3±0.1	74.6±0.1	74.3±0.3	72.9±0.3	71.6±0.4	70.5±0.4	79.2±0.2	77.1±0.3	+3.4
ASN	78.6±0.7	73.6±1.9	72.7±1.1	66.7±2.8	72.8±0.8	72.7±1.4	74.5±0.7	72.0±1.2	69.0±1.2	68.5±3.0	78.1±0.3	74.1±1.2	+1.6
GRADE	70.8±0.6	68.4±0.8	66.4±0.4	61.6±2.1	67.9±0.3	66.3±0.4	69.6±0.5	66.3±1.0	65.0±0.7	62.1±1.0	68.3±0.5	65.2±1.2	-4.7
StruRW	65.1±2.4	63.2±1.8	68.0±2.1	62.4±2.4	70.6±2.4	66.3±2.4	71.8±2.0	70.4±1.6	65.6±2.1	61.7±1.5	69.2±2.0	60.7±2.2	-4.9
SpecReg	67.5±1.6	64.3±2.3	66.4±1.4	61.8±2.3	68.7±1.4	65.2±3.1	71.8±1.0	65.9±2.1	65.9±1.5	58.8±3.8	67.0±1.8	58.9±1.7	-6.0
GraphAlign	73.2±1.1	70.1±1.1	67.5±1.4	64.6±1.2	67.2±1.1	66.6±1.1	71.6±1.1	68.2±1.8	59.6±1.6	58.8±1.0	66.0±0.8	62.9±1.7	-4.8
A2GNN	75.5±0.3	77.4±0.3	62.1±0.4	66.3±0.3	76.3±0.2	74.9±0.1	70.5±0.4	73.5±0.3	71.7±0.3	71.5±0.2	76.5±0.2	77.8±0.1	+1.7
GGDA-GCN	80.3±0.3	78.8±0.2	74.7±0.3	72.2±0.3	76.0±0.1	75.9±0.2	75.7±0.5	74.3±0.5	73.7±0.3	73.2±0.3	81.6±0.3	80.7±0.2	+5.3
GGDA-GAT	81.9±0.2	80.4±0.2	77.2±0.2	74.9±0.4	77.1±0.2	76.6±0.2	77.4±0.3	75.9±0.4	75.8±0.3	75.8±0.3	81.5±0.2	80.3±0.2	+6.7
GGDA-SAGE	78.0±0.3	76.8±0.3	72.4±0.6	70.0±0.5	75.6±0.2	75.6±0.3	74.1±0.5	72.3±0.7	70.8±0.3	71.3±0.4	76.3±0.5	76.0±0.5	+2.9
Oracle	97.3±0.1	96.9±0.1	96.9±0.1	96.8±0.1	97.0±0.1	97.0±0.1	96.9±0.1	96.8±0.1	97.0±0.1	97.0±0.1	97.3±0.1	96.9±0.1	

Table 2: Node classification accuracy on the target graph. OOM indicates out-of-memory errors.

					Arxiv 2007 to		To the last step of shift generation					Δ_{Mean}
	A2 to D2	D2 to A2	B1 to B2	B2 to B1	Arxiv 2016	Arxiv 2018	Cora	CiteSeer	ENGB	DE	PTBR	
CDAN	75.8±1.8	67.5±0.6	48.0±1.0	45.7±0.9	47.4±0.1	42.6±0.4	70.2±4.2	67.8±3.6	68.6±1.9	70.7±1.8	66.5±2.3	+0.6
MDD	74.2±1.5	69.8±1.3	44.0±0.7	43.5±0.8	45.8±0.5	52.3±1.3	59.2±1.7	64.1±3.2	65.6±4.2	67.9±2.2	65.9±0.4	-0.5
UDA-GCN	79.1±2.1	71.5±1.0	43.6±1.8	45.8±2.5	54.1±0.2	53.5±0.6	56.5±3.6	71.4±4.5	62.2±3.4	69.2±2.8	71.6±2.6	+1.3
ACDNE	70.1±1.4	60.3±1.5	53.1±1.3	51.3±1.3	43.5±0.6	40.9±1.3	60.4±3.9	53.6±3.1	50.8±2.7	56.8±2.6	68.1±2.2	-5.0
ASN	85.2±1.2	64.9±1.4	30.1±1.3	38.2±2.3	OOM	OOM	78.8±1.9	70.9±3.0	56.5±1.0	59.6±2.8	67.7±2.7	+0.9
GRADE	61.1±1.9	64.4±2.4	42.5±1.3	41.4±1.0	46.8±0.4	OOM	57.9±3.2	66.5±2.5	58.1±2.8	61.2±3.3	63.4±3.3	-4.1
StruRW	63.7±2.8	66.6±2.7	38.7±2.6	31.9±1.3	31.7±0.7	27.2±0.7	67.6±1.9	62.1±4.3	55.6±2.5	60.8±2.4	61.7±2.5	-8.8
SpecReg	75.6±6.9	68.0±2.0	44.7±1.0	43.7±1.0	53.2±0.5	47.6±1.9	72.0±4.3	75.6±3.7	68.1±3.6	69.7±1.4	69.5±1.2	+2.1
GraphAlign	67.8±1.4	68.0±1.6	45.1±1.2	45.9±0.4	30.1±0.3	27.5±0.7	61.0±2.4	56.2±5.2	69.4±3.8	69.9±4.8	67.8±2.0	-5.0
A2GNN	76.1±0.1	67.9±0.7	37.2±1.6	39.5±1.2	48.4±1.1	40.1±2.6	79.7±1.9	70.4±1.7	67.7±2.2	67.1±2.1	68.9±1.7	-0.1
GGDA-GCN	91.5±0.5	70.0±0.8	52.4±1.7	49.3±0.4	56.8±0.5	56.6±0.5	86.6±2.1	74.1±3.4	75.3±0.6	74.6±0.4	72.2±0.8	+8.7
GGDA-GAT	91.5±0.4	70.3±0.5	31.5±0.6	30.9±0.9	54.7±0.4	54.1±0.5	82.6±2.2	82.7±1.1	74.2±1.6	74.5±1.7	76.9±1.5	+5.4
GGDA-SAGE	78.5±0.6	58.2±0.5	50.2±1.0	50.3±1.0	55.0±0.1	53.2±0.4	87.4±1.2	83.6±1.1	61.8±1.2	64.8±1.0	70.5±0.9	+4.5
GGDA-GT	/	/	/	/	/	/	93.8±0.2	88.5±0.2	77.7±0.4	74.8±0.7	77.3±0.3	
Oracle	92.4±0.1	99.2±0.1	71.4±2.2	72.3±0.9	67.5±0.1	67.9±0.1	99.0±0.2	95.0±0.2	81.1±0.4	77.6±0.4	78.0±0.4	

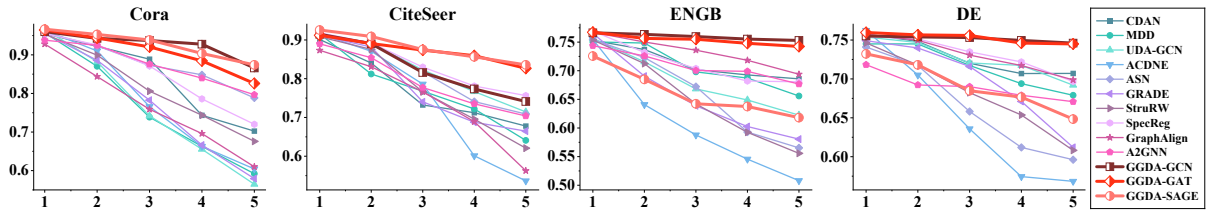


Figure 2: Node classification accuracy on target graphs with varying levels of discrepancy from the source graph. The x-axis shows the source-target discrepancy level ranked from 1 (closest) to 5 (farthest). The y-axis shows the classification accuracy.

multiple baselines incorporate advanced encoder designs to enhance transfer performance, for our GGDA framework, we focus on three fundamental encoders in this paper: GCN, GAT, and GraphSAGE [11, 17, 40]. Additionally, we include two baselines trained with ground-truth information. GGDA-GT performs GGDA on the ground-truth intermediate graphs from the *multi-step shifting process*, while Oracle is trained on a labeled target graph.

6.3 Result Analysis

6.3.1 Main Results. Table 1, Table 2 and Figure 2 present the performance of graph domain adaptations, with F1 scores for multi-label cases and accuracy scores for single-label cases. Δ_{Mean} in the tables indicates how a model’s performance compares to the mean performance across all models. For the *multi-step shifting* datasets, Table 2 shows the case where only the graph from the last step

Table 3: Performance drop in target graph node classifications across variants compared to the complete GGDA framework.

	A to D	D to C	C to A	A2 to D2	B1 to B2	Arxiv(07-16)	Arxiv(07-18)	CiteSeer	DE	PTBR	Avg. Drop
Source	-10.7±0.7	-11.0±0.9	-6.0±0.2	-17.0±0.9	-15.1±1.7	-5.6±0.9	-7.8±0.9	-15.8±4.9	-34.9±0.6	-37.2±1.1	-16.1
Direct ST	-6.7±0.6	-5.0±0.5	-3.2±0.3	-11.8±1.2	-11.2±2.4	-5.1±0.8	-7.6±1.1	-7.9±5.0	-7.3±6.4	-22.7±2.9	-8.9
DIR	-9.6±1.3	-13.1±1.2	-8.9±0.8	-11.1±3.5	-4.3±3.4	-4.3±1.0	-4.1±1.1	-21.2±6.5	-3.1±3.8	-6.6±1.4	-8.6
GGDA-I	-2.5±0.7	-5.2±0.6	-1.5±0.4	-7.5±2.6	-10.2±3.1	-2.1±1.0	-2.9±1.1	-4.1±7.1	-6.1±3.7	-4.7±4.1	-4.7
GGDA-R	-2.7±0.7	-1.3±0.7	-1.7±0.6	-0.7±0.6	-3.8±2.1	-2.0±0.5	-2.0±0.9	-2.0±5.9	-0.7±0.7	-1.5±1.0	-1.9

of shift generation is used as the target, while Figure 2 shows the case where graphs from each step of shift generation are treated as target graphs with different discrepancies from the source graph.

As shown in the tables, our proposed GGDA framework consistently outperforms other baselines given the intermediate domain construction that aims to minimize information loss upon adaptations and flexibly handles transfer scenarios with varied discrepancies. Moreover, the constructed domains effectively simulate the underlying data flow that bridges the gap, as evidenced by the small difference in target accuracy between our GGDA framework and GGDA-GT, which uses the actual intermediate data from the multi-step shifting process. Meanwhile, Figure 2 illustrates that GGDA-GCN and GGDA-GAT are the least susceptible to an increasing source-target discrepancy, and the high vulnerability of DIR-based models suggests that enforcing an alignment on domain distributions can lead to information distortion and backfire when the domain discrepancy is large. Such a limitation of DIR has also been theoretically validated in previous studies [51].

6.3.2 Ablation Studies. To investigate the effectiveness of different components, we conduct ablation studies as follows. (1) **Source**: direct transfer with a classifier trained on source; (2) **Direct ST**: self-training (i.e., iterative pseudo-labeling) without intermediate samples; (3) **DIR**: a prevalent graph DA framework with an adversarial domain classifier for distribution alignment; (4) **GGDA-I (Isolated)**: GGDA with each isolated graph $\tilde{\mu}_k$ as a separate domain; (5) **GGDA-R (Random)**: GGDA with a random matching function $m(\cdot)$ for graph generation. We adopt GCN in all cases, with the results shown in Table 3. Particularly, the significant performance drop of Direct ST and DIR highlights the crucial role of intermediate domains in exploiting the underlying data patterns for a robust graph DA. Meanwhile, DIR shows signs of negative transfer (i.e., lower accuracy than Source), underscoring the instability of domain alignment and its heavy reliance on additional model designs. The performance drop of GGDA-I validates the effectiveness of our dual modules in enhancing GGDA via the bonding of knowledge-preserving vertices and adaptive domain advancement, while the performance drop of GGDA-R reflects the improved information integrity from entropy-guided matching in graph generation.

6.3.3 Hyperparameter Analysis. The effects of κ and β are shown in Figure 3 and 4. From Figure 3, we observe that adjusting κ enables flexible domain constructions under varying inter-domain distance $W_p(\mu_t, \mu_{t+1})$ while maintaining an inverse relationship between the average distance Δ and the number of domains T . Meanwhile, Figure 4 shows that the optimal GGDA domain path occurs at a "sweet spot" when κ , and thus T , is not too small or too large, which aligns with the initial theoretical analysis. As for β , which governs the pace of weight decay, setting it to 0 equates to self-training on

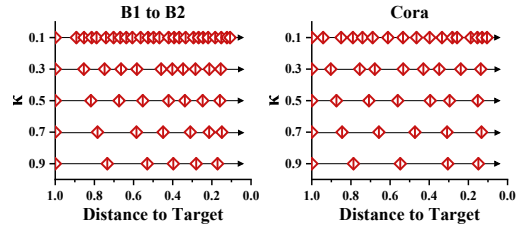


Figure 3: Progression of the constructed domain sequence under different κ . The x-axis shows the normalized embedding distance between the current and target domains.

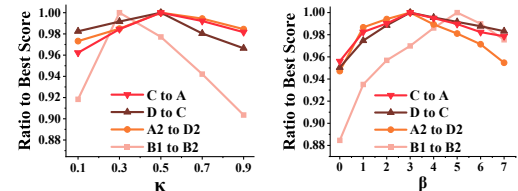


Figure 4: Performance of our GGDA framework with varying values of hyperparameters κ and β .

the entire graph sequence without considering distribution shifts, while an overly large β causes rapid information decay before full utilization, both of which can deteriorate transfer performance.

6.3.4 Runtime Comparison. Table 4 compares the model efficiency on transfer Arxiv(07-18), the largest dataset. All models are trained until convergence at either around 1000 or 200 epochs. Our GGDA framework achieves a runtime comparable to other models while significantly improving target predictions. Despite the non-generative nature of DIR models, they rely heavily on advanced encoder designs and regularizations, leading to costly computations such as eigendecomposition and topological matching. As for GraphAlign, a data-centric method, the graph generation is computationally intensive when the generated graph exceeds 1% of the target graph size, i.e., a huge trade-off between time and performance. Overall, our novel GGDA framework strikes an optimal balance via the accelerated graph generation technique and the careful domain constructions that attain minimal transfer information loss.

7 Related Works

Graph Domain Adaptation. A popular framework for node-level graph domain adaptation is to perform adversarial training and learn domain-invariant representations that fool the domain discriminator [2, 4, 10, 20–22, 25, 29, 33, 34, 42–45, 48, 50]. Approaches

Table 4: Comparison of runtime on Arxiv(07-18) (for 1000 epochs) and average performance score across all datasets.

Model	Runtime (seconds)	Avg. Score
SpecReg	532.3	63.9
A2GNN	643.6	66.8
ACDNE	1849.9 (for 200 epochs)	65.4
GraphAlign	1422.7 (for 200 epochs)	61.1
GGDA-GCN	668.2 (graph generation)	72.9
	+ 208.5 (domain progression) = 876.7	

based on ego-graph information maximization [54], spectral regularization that modulates the GNN Lipschitz constant for error bounding [47], and generation of new source graph [15] have also been proposed. However, none of these works have addressed the critical scenario of a large distribution gap.

Intermediate Domains for IID Domain Adaptation. The use of intermediate domains has shown promise in addressing IID domain adaptation tasks [1, 3, 7, 9, 12, 13, 18, 26, 28, 36, 41, 46, 52]. To generate intermediate domains, some works construct them as generative subspaces [7, 9], while other works generate them on a sample level [1, 8, 12, 26, 46]. A line of research that leverages a sequence of intermediate domains is gradual domain adaptation (GDA) [1, 3, 12, 18, 31, 35, 41]. However, the effect of intermediate domains and GDA in a non-IID graph context is still under-explored.

8 Conclusion

This work presents a pioneering effort to tackle a significant source-target graph discrepancy and to establish a graph gradual domain adaptation (GGDA) framework. We propose efficient FGW-based generation of knowledge-preserving intermediate graphs for bridging the gap, upon which we develop vertex-based domain constructions that approach the shortest adaptation path via information loss minimization. Our framework bounds the target generalization error by establishing implementable lower and upper bounds of $W_p(\mu_t, \mu_{t+1})$, an intractable metric in the graph context. Future work may explore GGDA extensions tailored to specific scenarios.

References

- [1] Samira Abnar, Rianne van den Berg, Golnaz Ghiasi, Mostafa Dehghani, Nal Kalchbrenner, and Hanie Sedghi. 2021. Gradual domain adaptation in the wild: When intermediate distributions are absent. *arXiv preprint arXiv:2106.06080* (2021).
- [2] Ruichu Cai, Fengzhu Wu, Zijian Li, Pengfei Wei, Lingling Yi, and Kun Zhang. 2024. Graph domain adaptation: A generative view. *ACM Transactions on Knowledge Discovery from Data* 18, 3 (2024), 1–24.
- [3] Hong-You Chen and Wei-Lun Chao. 2021. Gradual domain adaptation without indexed intermediate domains. *Advances in neural information processing systems* 34 (2021), 8201–8214.
- [4] Quanyu Dai, Xiao-Ming Wu, Jiaren Xiao, Xiao Shen, and Dan Wang. 2022. Graph transfer learning via adversarial domain adaptation with graph convolution. *IEEE Transactions on Knowledge and Data Engineering* 35, 5 (2022), 4908–4922.
- [5] Cornelia Drutu and Michael Kapovich. 2018. *Geometric group theory*. Vol. 63. American Mathematical Soc.
- [6] Yaroslav Ganin, Evgeniya Ustinova, Hana Ajakan, Pascal Germain, Hugo Larochelle, François Laviolette, Mario March, and Victor Lempitsky. 2016. Domain-adversarial training of neural networks. *Journal of machine learning research* 17, 59 (2016), 1–35.
- [7] Boqing Gong, Yuan Shi, Fei Sha, and Kristen Grauman. 2012. Geodesic flow kernel for unsupervised domain adaptation. In *2012 IEEE conference on computer vision and pattern recognition*. IEEE, 2066–2073.
- [8] Rui Gong, Wen Li, Yuhua Chen, and Luc Van Gool. 2019. Dlow: Domain flow for adaptation and generalization. In *Proceedings of the IEEE/CVF conference on computer vision and pattern recognition*. 2477–2486.
- [9] Raghuraman Gopalan, Ruonan Li, and Rama Chellappa. 2011. Domain adaptation for object recognition: An unsupervised approach. In *2011 international conference on computer vision*. IEEE, 999–1006.
- [10] Gaoyang Guo, Chaokun Wang, Bencheng Yan, Yunkai Lou, Hao Feng, Junchao Zhu, Jun Chen, Fei He, and S Yu Philip. 2022. Learning adaptive node embeddings across graphs. *IEEE Transactions on Knowledge and Data Engineering* 35, 6 (2022), 6028–6042.
- [11] Will Hamilton, Zhitao Ying, and Jure Leskovec. 2017. Inductive representation learning on large graphs. *Advances in neural information processing systems* 30 (2017).
- [12] Yifei He, Haoxiang Wang, Bo Li, and Han Zhao. 2023. Gradual Domain Adaptation: Theory and Algorithms. *arXiv preprint arXiv:2310.13852* (2023).
- [13] Han-Kai Hsu, Chun-Han Yao, Yi-Hsuan Tsai, Wei-Chih Hung, Hung-Yu Tseng, Maneesh Singh, and Ming-Hsuan Yang. 2020. Progressive domain adaptation for object detection. In *Proceedings of the IEEE/CVF winter conference on applications of computer vision*. 749–757.
- [14] Weihua Hu, Matthias Fey, Marinka Zitnik, Yuxiao Dong, Hongyu Ren, Bowen Liu, Michele Catasta, and Jure Leskovec. 2020. Open graph benchmark: Datasets for machine learning on graphs. *Advances in neural information processing systems* 33 (2020), 22118–22133.
- [15] Renhong Huang, Jiarong Xu, Xin Jiang, Ruichuan An, and Yang Yang. 2024. Can Modifying Data Address Graph Domain Adaptation?. In *Proceedings of the 30th ACM SIGKDD Conference on Knowledge Discovery and Data Mining*. 1131–1142.
- [16] George Karypis and Vipin Kumar. 1998. A fast and high quality multilevel scheme for partitioning irregular graphs. *SIAM Journal on scientific Computing* 20, 1 (1998), 359–392.
- [17] Thomas N Kipf and Max Welling. 2016. Semi-supervised classification with graph convolutional networks. *arXiv preprint arXiv:1609.02907* (2016).
- [18] Ananya Kumar, Tengyu Ma, and Percy Liang. 2020. Understanding self-training for gradual domain adaptation. In *International conference on machine learning*. PMLR, 5468–5479.
- [19] Jundong Li, Xia Hu, Jiliang Tang, and Huan Liu. 2015. Unsupervised streaming feature selection in social media. In *Proceedings of the 24th ACM International Conference on Information and Knowledge Management*. 1041–1050.
- [20] Meihan Liu, Zeyu Fang, Zhen Zhang, Ming Gu, Sheng Zhou, Xin Wang, and Jiajun Bu. 2024. Rethinking Propagation for Unsupervised Graph Domain Adaptation. *arXiv preprint arXiv:2402.05660* (2024).
- [21] Shikun Liu, Tianchun Li, Yongbin Feng, Nhan Tran, Han Zhao, Qiang Qiu, and Pan Li. 2023. Structural re-weighting improves graph domain adaptation. In *International Conference on Machine Learning*. PMLR, 21778–21793.
- [22] Shikun Liu, Deyu Zou, Han Zhao, and Pan Li. 2024. Pairwise Alignment Improves Graph Domain Adaptation. *arXiv preprint arXiv:2403.01092* (2024).
- [23] Mingsheng Long, Zhangjie Cao, Jianmin Wang, and Michael I Jordan. 2018. Conditional adversarial domain adaptation. *Advances in neural information processing systems* 31 (2018).
- [24] Mingsheng Long, Han Zhu, Jianmin Wang, and Michael I Jordan. 2017. Deep transfer learning with joint adaptation networks. In *International conference on machine learning*. PMLR, 2208–2217.
- [25] Yuzhen Mao, Jianhui Sun, and Dawei Zhou. 2022. Augmenting Knowledge Transfer across Graphs. In *2022 IEEE International Conference on Data Mining (ICDM)*. IEEE, 1101–1106.
- [26] Jaemin Na, Heechul Jung, Hyung Jin Chang, and Wonjun Hwang. 2021. Fixbi: Bridging domain spaces for unsupervised domain adaptation. In *Proceedings of the IEEE/CVF conference on computer vision and pattern recognition*. 1094–1103.
- [27] Sinno Jialin Pan and Qiang Yang. 2009. A survey on transfer learning. *IEEE Transactions on knowledge and data engineering* 22, 10 (2009), 1345–1359.
- [28] Gabriel Peyré, Marco Cuturi, et al. 2019. Computational optimal transport: With applications to data science. *Foundations and Trends® in Machine Learning* 11, 5-6 (2019), 355–607.
- [29] Ziyue Qiao, Xiao Luo, Meng Xiao, Hao Dong, Yuanchun Zhou, and Hui Xiong. 2023. Semi-supervised domain adaptation in graph transfer learning. *arXiv preprint arXiv:2309.10773* (2023).
- [30] Benedek Rozemberczki, Carl Allen, and Rik Sarkar. 2021. Multi-scale attributed node embedding. *Journal of Complex Networks* 9, 2 (2021), cnab014.
- [31] Shogo Sagawa and Hideitsu Hino. 2022. Gradual domain adaptation via normalizing flows. *arXiv preprint arXiv:2206.11492* (2022).
- [32] Prithviraj Sen, Galileo Namata, Mustafa Bilgic, Lise Getoor, Brian Galligher, and Tina Eliassi-Rad. 2008. Collective classification in network data. *AI magazine* 29, 3 (2008), 93–93.
- [33] Xiao Shen, Quanyu Dai, Fu-lai Chung, Wei Lu, and Kup-Sze Choi. 2020. Adversarial deep network embedding for cross-network node classification. In *Proceedings of the AAAI conference on artificial intelligence*, Vol. 34. 2991–2999.
- [34] Boshen Shi, Yongqing Wang, Fangda Guo, Jiangli Shao, Huawei Shen, and Xueqi Cheng. 2023. Improving graph domain adaptation with network hierarchy. In *Proceedings of the 32nd ACM International Conference on Information and*

- Knowledge Management*. 2249–2258.
- [35] Lianghe Shi and Weiwei Liu. 2024. Adversarial Self-Training Improves Robustness and Generalization for Gradual Domain Adaptation. *Advances in Neural Information Processing Systems* 36 (2024).
- [36] Ben Tan, Yu Zhang, Sinno Pan, and Qiang Yang. 2017. Distant domain transfer learning. In *Proceedings of the AAAI conference on artificial intelligence*, Vol. 31.
- [37] Vayer Titouan, Nicolas Courty, Romain Tavenard, and Rémi Flamary. 2019. Optimal transport for structured data with application on graphs. In *International Conference on Machine Learning*. PMLR, 6275–6284.
- [38] Eric Tzeng, Judy Hoffman, Kate Saenko, and Trevor Darrell. 2017. Adversarial discriminative domain adaptation. In *Proceedings of the IEEE conference on computer vision and pattern recognition*. 7167–7176.
- [39] Titouan Vayer, Laetitia Chapel, Rémi Flamary, Romain Tavenard, and Nicolas Courty. 2020. Fused Gromov-Wasserstein distance for structured objects. *Algorithms* 13, 9 (2020), 212.
- [40] Petar Veličković, Guillem Cucurull, Arantxa Casanova, Adriana Romero, Pietro Lio, and Yoshua Bengio. 2017. Graph attention networks. *arXiv preprint arXiv:1710.10903* (2017).
- [41] Haoxiang Wang, Bo Li, and Han Zhao. 2022. Understanding gradual domain adaptation: Improved analysis, optimal path and beyond. In *International Conference on Machine Learning*. PMLR, 22784–22801.
- [42] Yu Wang, Ronghang Zhu, Pengsheng Ji, and Sheng Li. 2024. Open-Set Graph Domain Adaptation via Separate Domain Alignment. In *Proceedings of the AAAI Conference on Artificial Intelligence*, Vol. 38. 9142–9150.
- [43] Jun Wu, Jingrui He, and Elizabeth Ainsworth. 2023. Non-iid transfer learning on graphs. In *Proceedings of the AAAI Conference on Artificial Intelligence*, Vol. 37. 10342–10350.
- [44] Man Wu, Shirui Pan, Chuan Zhou, Xiaojun Chang, and Xingquan Zhu. 2020. Unsupervised domain adaptive graph convolutional networks. In *Proceedings of The Web Conference 2020*. 1457–1467.
- [45] Man Wu, Shirui Pan, and Xingquan Zhu. 2022. Attraction and repulsion: Unsupervised domain adaptive graph contrastive learning network. *IEEE Transactions on Emerging Topics in Computational Intelligence* 6, 5 (2022), 1079–1091.
- [46] Minghao Xu, Jian Zhang, Bingbing Ni, Teng Li, Chengjie Wang, Qi Tian, and Wenjun Zhang. 2020. Adversarial domain adaptation with domain mixup. In *Proceedings of the AAAI conference on artificial intelligence*, Vol. 34. 6502–6509.
- [47] Yuning You, Tianlong Chen, Zhangyang Wang, and Yang Shen. 2023. Graph domain adaptation via theory-grounded spectral regularization. In *The eleventh international conference on learning representations*.
- [48] Xiaowen Zhang, Yuntao Du, Rongbiao Xie, and Chongjun Wang. 2021. Adversarial separation network for cross-network node classification. In *Proceedings of the 30th ACM international conference on information & knowledge management*. 2618–2626.
- [49] Yuchen Zhang, Tianle Liu, Mingsheng Long, and Michael Jordan. 2019. Bridging theory and algorithm for domain adaptation. In *International conference on machine learning*. PMLR, 7404–7413.
- [50] Yizhou Zhang, Guojie Song, Lun Du, Shuwen Yang, and Yilun Jin. 2019. Dane: Domain adaptive network embedding. *arXiv preprint arXiv:1906.00684* (2019).
- [51] Han Zhao, Remi Tachet Des Combes, Kun Zhang, and Geoffrey Gordon. 2019. On learning invariant representations for domain adaptation. In *International conference on machine learning*. PMLR, 7523–7532.
- [52] Jun-Yan Zhu, Taesung Park, Phillip Isola, and Alexei A Efros. 2017. Unpaired image-to-image translation using cycle-consistent adversarial networks. In *Proceedings of the IEEE international conference on computer vision*. 2223–2232.
- [53] Meiqi Zhu, Xiao Wang, Chuan Shi, Houye Ji, and Peng Cui. 2021. Interpreting and unifying graph neural networks with an optimization framework. In *Proceedings of the Web Conference 2021*. 1215–1226.
- [54] Qi Zhu, Carl Yang, Yidan Xu, Haonan Wang, Chao Zhang, and Jiawei Han. 2021. Transfer learning of graph neural networks with ego-graph information maximization. *Advances in Neural Information Processing Systems* 34 (2021), 1766–1779.